

# One-dimensional model of cardiac defibrillation

R. Plonsey<sup>1</sup> R. C. Barr<sup>1</sup> F. X. Witkowski<sup>2</sup>

<sup>1</sup>Department of Biomedical Engineering  
Duke University, Durham, North Carolina, NC 27706, USA

<sup>2</sup>University of Alberta, Edmonton, Canada

**Abstract**—The response of a single strand of cardiac cells to a uniform defibrillatory shock assuming steady-state linear conditions is examined. It is argued that the effect of this current is quantitatively described by the induced transmembrane potential even under passive conditions. The characteristics of the single strand are those that would exist if the heart was a system of equivalent parallel pathways from apex to base. It is shown that essentially every cell is both hyperpolarised and depolarised from the shock by an amount proportional to the stimulus intensity and the intercellular junctional resistance. For physiological values of model parameters the evaluated depolarisations are consistent with levels necessary to affect electrophysiological behaviour.

**Keywords**—Cardiac cells, Defibrillation

Med. & Biol. Eng. & Comput., 1991, 29, 465–469

## 1 Introduction

PLONSEY AND BARR (1986*a*; *b*) examined the response of a one-dimensional model of cardiac tissue to a defibrillatory current pulse to quantitatively evaluate those factors which affect the induced transmembrane potential. Their motivation was based on an understanding that the ability of a defibrillatory current to terminate fibrillation can only be explained as the response to the induced transmembrane potential. (That is, cell behaviour can only be altered by an external current if a modification in the transmembrane potential is produced.) The simulations were performed on a single equivalent cardiac strand consisting of 30 coupled cells subject to an applied voltage at the ends. If the heart were truly uniform, isotropic and syncytial, the response to a defibrillating field established by parallel electrodes at the apex and base could be examined through a prototypical single fibre path such as that considered here. The model parameters include intra- and extracellular axial resistance, membrane resistance and intercellular junctional resistance and are based on assumed linear steady-state conditions. The resulting transmembrane potential  $v_m$  shown in Fig. 1, arises from insertion of nominal values for the aforementioned resistances and a nominal value of defibrillating current, as described in PLONSEY and BARR (1986*a*), and is based on an assumed 30 cell length equivalent fibre. In this plot the solid curve shows an average behaviour characteristic of a uniform fibre. Fluctuations arising from the presence of the discrete junctions are superimposed (dotted curve).

A steady-state model is considered even though the phenomenon of interest is basically time-varying and supra-threshold. In some ways, the presence of membrane

capacitance, ignored in this model, may be regarded to introduce effects comparable to those of lowering of the membrane resistance. As will be seen, the magnitude of  $v_m$  should be relatively unaffected by this. Furthermore, the resting membrane time constant is of the same order of magnitude as a typical defibrillatory shock duration (6–10 ms) so that, in fact, near steady-state conditions could be reached. To the degree that there is nonlinear membrane behaviour,  $v_m$  will differ from what is evaluated here.

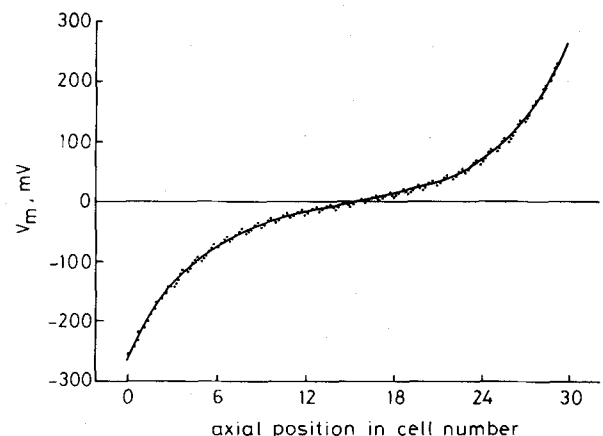


**Fig. 1** The variation in steady-state subthreshold transmembrane potential  $v_m$  along an equivalent cardiac strand consisting of 30 cells subjected to an applied current of  $0.05 \mu\text{A}$  through extracellular electrodes at the ends, simulating defibrillatory conditions. Resistance values reflecting nominally normal cardiac muscle are  $r_i = 1.98 \text{ M}\Omega \text{ cell}^{-1}$ ,  $r_e = 1.14 \text{ M}\Omega \text{ cell}^{-1}$ ,  $r_m = 84.9 \text{ M}\Omega \text{ cell}^{-1}$ , and  $R_j$  (junctional resistance) =  $849 \text{ k}\Omega \text{ cell}^{-1}$ . The cell length is  $125 \mu\text{m}$ . The continuous line shows the result when the junctional resistance is included as part of a continuous intracellular resistance, the dotted curve recognises the discrete nature of the junctional resistance

Correspondence should be addressed to Dr Robert Plonsey.

First received 10th May and in final form 20th August 1990

© IFMBE: 1991

Still, the steady-state  $v_m$  can be thought to describe the relative membrane response (modification) to an applied current. Thereby it should be a measure of the ability of the stimulus to affect the electrophysiological behaviour of the membrane. Thus, the model achieves the benefit of a substantial simplification, yet preserves a first-order estimate of the desired effect.

As already noted, in previous work (PLONSEY and BARR, 1986a), a fibre length composed of 30 cells was selected, loosely based on the idea that nonuniformities in cardiac tissue effectively break up the heart into smaller regions. However, a review of the current literature suggests that even where connective tissue and collagenous septa are dense they do not interfere with longitudinal currents (DOLBER and SPACH, 1987). According to these data, it may be concluded that defibrillatory currents entering the heart will follow a continuous fibre path that is uninterrupted from one end to the other. A typical path from apex to base, which is nominally 15 cm in length for a human heart, can be identified using the work of STREETER (1979). This equivalent fibre contains 1200 cells, each of length 125  $\mu\text{m}$ , and comprises the simplified model to be considered. (For simplicity, its possible helical shape (STREETER, 1979) is ignored.) For a typical internal defibrillatory voltage of 300V an average field strength of 20V  $\text{cm}^{-1}$  results, which is in the range cited by IDEKER *et al.* (1987) and WITKOWSKI *et al.* (1990) for successful defibrillation.

Although earlier papers (PLONSEY and BARR, 1986a; b) could be modified by simply replacing the 30 cells by 1200 cells, and the basic implication of this change is not difficult to deduce from those papers, we thought it would be useful to start afresh with simplifications introduced from the outset. In this way the factors and possible mechanism for defibrillation can be readily evaluated quantitatively, and their implications emphasised and appreciated.

The following sections develop a mathematical expression for the transmembrane potential changes to be expected within a cell that is away from the ends of a long chain of cells. This expression is remarkable in that it can be obtained without evaluating the voltages and currents on the fibre as a whole. From reported values of relevant parameters, we obtain a quantitative estimate of the transmembrane potential which is expected from a defibrillatory pulse in a fibre at rest. Other results suggest that the calculations are a reasonable measure of the impact of the stimulus under active conditions.

## 2 Model

An experimental determination of the space constant\*  $\lambda$  for a one-dimensional cardiac strand typically shows  $\lambda$  to lie within a range of 3–10 cells (CHAPMAN and FRY, 1978). For the data on which Fig. 1 is based,  $\lambda = 5.2$  cells or 650  $\mu\text{m}$ . If the aforementioned equivalent cardiac fibre of length 15 cm is continuous and an electrode was placed at both ends, an applied subthreshold current would redistribute between the interstitial and intracellular spaces only near each end (according to linear core-conductor theory (WEIDMANN, 1970)). Redistribution would be essentially complete at a distance of a few space constants from each end. If we characterise this region as  $5\lambda$  or 3 mm in length, over the remaining 14.4 cm of the equivalent fibre, which is essentially the entire fibre, the intracellular and

interstitial current would be constant and the net transmembrane current concomitantly zero. In this uniform zone, the relative proportion of intracellular axial current  $I_i$  and interstitial axial current  $I_e$  is given by

$$\frac{I_e}{I_i} = \frac{r_i}{r_e} \quad (1)$$

where  $r_e$  and  $r_i$  are the respective axial resistances per unit length. Eqn. 1 can be recognised as an expression for the division of the total axial current into components which are inversely proportional to the axial resistances; this condition maintains the requirement of zero transmembrane current.

If the individual cells and their junctional coupling resistance are now recognised, the above description will still be correct but only in an averaged way. One must now evaluate an averaged intracellular axial resistance per unit length  $r'_i$  which includes the junctional resistance  $R_j$  per cell; this averaged resistance is given by  $r'_i = r_i + R_j/l$ , where  $l$  is the cell length. Under these conditions, eqn. 1 describes the average magnitude of the axial currents provided  $r_i$  is replaced by  $r'_i$ .

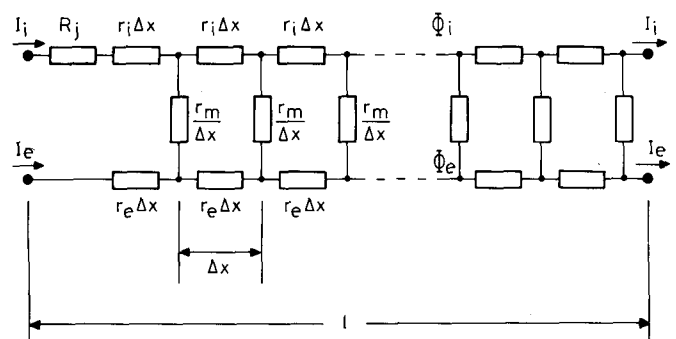


Fig. 2 Electrical model of a single interior cardiac cell and its intercellular connection to its neighbouring cells. The junctional resistance  $R_j$  is essentially lumped (or discrete). The resistances per elementary length  $\Delta x$  within the cell are  $r_i \Delta x$ ,  $r_e \Delta x$  and  $r_m \Delta x$ . As usual,  $r_i$  and  $r_e$  are the intracellular and extracellular axial resistance per unit length and  $r_m$  is the membrane resistance times length. An infinite number of infinitesimal elements within the cell is shown as a way of characterising the region as a continuum

An electrical description of an interior cell is shown in Fig. 2. It describes the steady-state behaviour of around 98 per cent of the cells in the fibre based on the aforementioned comments. The requirement that each interior cell of the chain of 1200 cells behave identically means that  $I_e$  and  $I_i$  must have the same values at points exactly one cell length apart. That is, these currents must be spatially repetitive with a periodicity of exactly one cell length. The transmembrane current per unit length  $i_m$  must have an average value of zero, but it is only necessary that a zero average arises for an integration taken over exactly one cell length; within a cell-length an inflow and compensating outflow is permitted. In fact, because of the presence of the discrete junctional resistance  $R_j$ , nonzero inflows and outflows are required, even though the average is zero.

With reference to Fig. 2, it is clear that a discontinuity in the intracellular potential  $\Phi_i$  will, in fact, be introduced by the discrete junctional resistance. For the directions of current shown, the membrane will be hyperpolarised just to the right of the junction resulting from the IR drop of  $I_i R_j$ . As a consequence of this voltage there will be an inward membrane current over the left-hand portion of the cell. Conversely, over the right-hand side of the cell the original axial currents must be restored to satisfy the

\* The space constant for the linear core conductor model of Fig. 1 is  $\lambda = \sqrt{r_m / (r_i + r_e)}$  and is a measure of the distance over which the response to a stimulating current step will be observed (PLONSEY and BARR, 1988).

aforementioned periodicity. Based on symmetry, the right-hand side of the cell will be the site of an outward current (and a transmembrane depolarisation) that exactly compensates for the inward currents on the left, so the average is zero.

The behaviour of currents and potentials within the cell are continuous and must satisfy the classical cable equations (PLONSEY and BARR, 1988). Under steady-state conditions, the governing partial differential equation for the transmembrane potential  $v_m$  is (PLONSEY and BARR, 1988)

$$\lambda^2 \frac{d^2 v_m}{dx^2} - v_m = 0 \quad (2)$$

If the centre of the cell is chosen as the origin for the axial co-ordinate  $x$ , solutions to eqn. 2 must be antisymmetric, and will necessarily involve a hyperbolic sine function. One can construct the solution to eqn. 2 which satisfies the boundary conditions described above as

$$v_m(x) = \frac{I_0 R_j r_e}{2(r_i + r_e + R_j/l)} \frac{\sinh(x/\lambda)}{\sinh(l/2\lambda)} \quad (3)$$

Eqn. 3 is only valid for  $-l/2 \leq x \leq l/2$ , however, it describes the response within each and every cell. Consequently a discontinuity in  $v_m$  will occur at the junction between every cell.

Note that  $v_m(x)$  is correctly antisymmetric, satisfies eqn. 2 and is discontinuous by the magnitude  $I_i R_j$  at each end, where  $I_i = I_0 r_e / (r_e + r_i + R_j/l)$ . In eqn. 3  $I_0$  denotes the portion of the total applied, defibrillatory current associated with the fibre under consideration. The intracellular current is obtained from it by the application of eqn. 1 using  $r_i$  and noting that conservation of current requires that  $I_0 = I_i + I_e$ . If the heart cross-sectional area is  $A$ , the cell radius is  $a$ , the interstitial space is a fraction  $f$  of the intracellular space and  $I_T$  is the actual total current applied directly to the heart for defibrillation, we can approximate

$$I_0 = \frac{(1+f)\pi a^2 I_T}{A} \quad (4)$$

Eqn. 4 is crude and introduced mainly for illustrative purposes. It is based on the simplifying assumption that the total current is uniformly distributed within the entire heart, so that the amount associated with an equivalent single fibre is proportional to its cross-sectional area relative to the total area. The use of typical values, as discussed by PLONSEY and BARR (1986a), gives  $I_0 = 0.05 \mu A$  based on  $I_T = 10 A$  or a transthoracic current of perhaps 50 A. This includes a reduction of  $I_0$  by a factor of five to compensate for possible spatial variations in current density through the heart cross-section as well as current which does not pass through the heart at all. This compensatory factor is probably high, and therefore the ultimate results should be viewed as quite conservative.

### 3 Transmembrane voltage

A plot of the variation of transmembrane potential, described by eqn. 3, over four consecutive interior cells is shown in Fig. 3. The cardiac resistance values used are nominally normal ones as described by PLONSEY and BARR (1986a); the actual data are the same as those for Fig. 1 which are given in that figure caption. Note that the curves satisfy the requirement that field quantities are spatially periodic, and that the average value of  $v_m$  is zero. As steady-state conditions are assumed  $i_m = v_m/r_m$ , consequently  $i_m$  also averages to zero over any cell length as required.

It is also noted that the expected hyperpolarisation at the left-hand side of each cell and symmetrical depolarisation on the right-hand side does indeed occur. One might wonder how the picture is altered if cells in a particular region are undergoing depolarisation or fibrillation. The

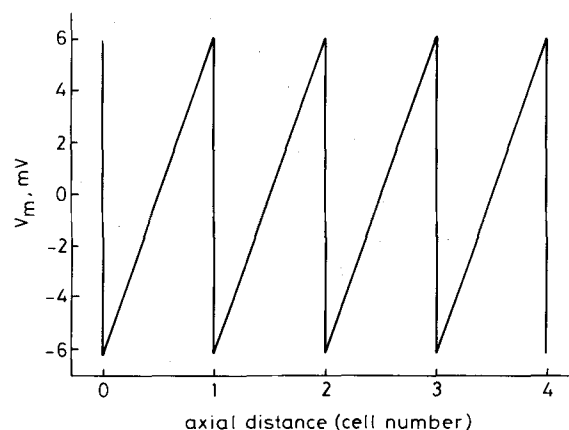


Fig. 3 The transmembrane potential for four consecutive interior cells (total number of cells is 2400), thereby justifying the use of eqn. 3. The values assigned to  $r_i$ ,  $r_e$ ,  $r_m$  and  $R_j$  are nominally normal for cardiac tissue and are given in the caption of Fig. 1

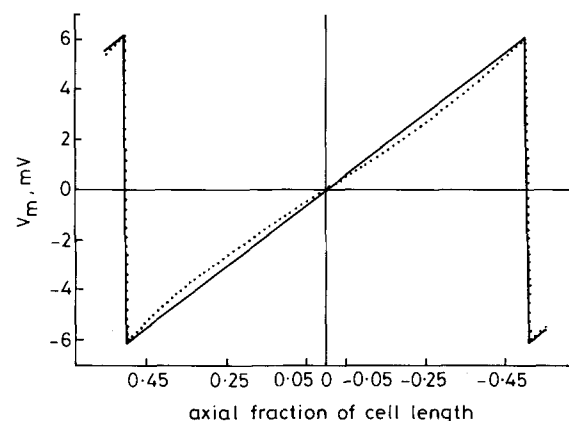


Fig. 4 The variation of transmembrane potential within a single interior cell is shown for the normal value of  $r_m = 84.9 M\Omega \text{ cell}^{-1}$  (solid line) and  $r_m = 0.849 M\Omega \text{ cell}^{-1}$  (dotted curve). For the normal case  $\lambda = 650 \mu m$  and in the latter case  $\lambda = 65 \mu m$  (i.e. one-tenth the normal value). Note that the abscissa is the axial distance normalised to the cell length. That is, if  $X$  is the value of the abscissa in this figure, then  $X = x/l$ , where  $x$  is the actual dimension as appears in eqn. 3 and  $l$  is the cell length

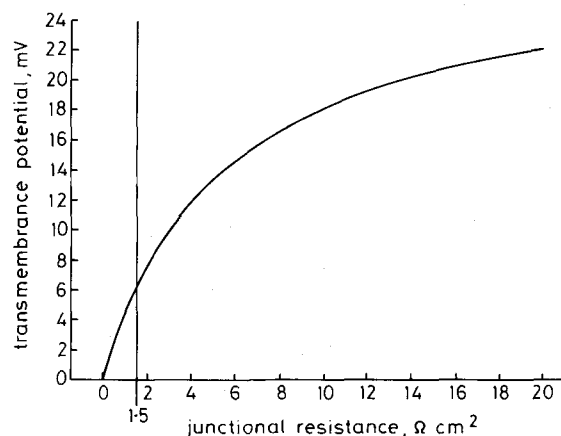


Fig. 5 The peak value of hyper- and depolarisation within each cell is shown as a function of junctional resistance in  $\Omega \text{ cm}^2$ . The nominally normal value of  $R_j = 1.5 \Omega \text{ cm}^2$  is indicated, and corresponds to the junctional resistance used in Fig. 1 and Fig. 3. Other resistance values are as given in the caption to Fig. 1

main effect appears to be a reduction in the magnitude of membrane resistance because all other quantities affecting eqn. 3 are nominally unchanged. A change in the magnitude of  $r_m$  will affect the value of  $\lambda$ . If we assume a reduction of  $r_m$  by two orders of magnitude, the value of  $\lambda$  will diminish to one-tenth. The potential variation over a single cell in Fig. 3 is replotted in Fig. 4 and compared with the curve that results with  $\lambda$  diminished by one-tenth. The maximum magnitude of hyper- and depolarisation is unchanged, but the shape of the transmembrane potential curve is modified. The effect, however, appears to be quite modest. Of course, in a diseased heart, a region that has become ischemic may have an increased value of  $R_j$  and possibly the values of  $r_i$  and  $r_e$  will be modified as well. Finally, in Fig. 5, we show the dependence of the magnitude of hyper- and depolarisation on the junctional resistance  $R_j$  as expressed in eqn. 3. In Fig. 5  $R_j$  is described in units of  $\Omega \text{ cm}^2$ , as usual. Recent electrophysiological studies put the value of  $R_j$  somewhere in the range of  $1\text{--}4 \Omega \text{ cm}^2$  (CHAPMAN and FRY, 1978).

#### 4 Discussion

In spite of the simplicity of both the model and the derivation of eqn. 3, the resulting description of cellular behaviour in the heart due to a defibrillatory impulse is interesting and possibly significant. We list some consequences below:

- (i) Eqn. 3 applies to every cardiac cell not near the surface, therefore each and every cell will be both hyperpolarised and depolarised by a defibrillatory shock. The electrophysiological consequences have not been studied, but if fibrillation is characterised by calcium action potentials (HESCHELER and SPEICHER, 1989) this could constitute an adequate stimulus to elicit a normal sodium action potential. Possibly such an (sodium) activation could occur regardless of the phase in which a cell finds itself at the moment of introduction of a defibrillatory shock and hence would occur in each cell. On the other hand, for defibrillation to result, it may be sufficient that cellular behaviour is modified (i.e. action potentials prolonged) so that a probable re-entrant loop is interfered with. That the model demonstrates a stimulus at all cells seems consistent with the finding that a substantial (critical) mass of tissue is affected in a successful defibrillation (WITKOWSKI *et al.*, 1990). (The anode is on the right and the cathode on the left.)
- (ii) The magnitude of both hyper- and depolarisation, based on nominal cardiac electrophysiological values, is in the range of 10 mV, as described by Fig. 5. Consequently, it is in the 'ball-park' for affecting cellular behaviour. Further, as the value of  $I_0$  is conservative, a greater value of induced transmembrane potential is likely.
- (iii) The magnitude of hyper- and depolarisation appears to be independent of whether the cell is in the resting or active state. Consequently, a 'stimulus' is supplied to all cells regardless of their exact electrical phase and condition. When this is considered, along with eqns. 1 and 2 above, successful defibrillation could be explained as resulting from the simultaneous modification in the behaviour of a very large number of cells in the heart.
- (iv) The effect of cellular decoupling is to increase  $R_j$  and hence the strength of a defibrillatory stimulus.
- (v) According to the model, the behaviour of all cells is unaffected by a reversal in the polarity of the elec-

trodes. Clinical studies support this conclusion because the differences seen are not great (SCHUDER *et al.*, 1987). Real cells are not symmetrical, as assumed in Fig. 2, and so to this extent a different response may be elicited by a reversal of polarity.

- (vi) For a heart at rest, activation (not defibrillation) requires that some (any) region is depolarised. As the cells near the electrodes (ignored here, but see PLONSEY and BARR (1986a; b)) undergo larger hyper- and depolarisation, excitatory currents one or two orders of magnitude smaller should be successful. Indeed it is noted in practice that current levels for activation are roughly an order of magnitude smaller than those required for defibrillation (IDEKER *et al.*, 1987).
- (vii) The optimum distribution of defibrillation currents throughout the heart should be uniform. This ensures that  $I_0$  in eqn. 3 is the same for all cells because one cannot *a priori* identify any particular region in which a greater (or lesser) current density is preferred. This conclusion corresponds to the 'conventional wisdom'.

#### 5 Conclusions

The induced transmembrane potential in all heart cells, regardless of their electrophysiological state, from a conventional defibrillatory pulse, appears to be in the range of 10–100 mV. On this basis it is suggested that defibrillation is successful through the modification of prior electrical behaviour and the initiation of a new pattern of activity at a very large number of sites. This is also the conclusion in the study by WITKOWSKI *et al.* (1990), with which this model is consistent. Clearly, further study is needed regarding the electrophysiological response of a cell to simultaneous hyper- and depolarisation and its consequences for re-entry. In this latter study the inclusion of membrane capacitance as well as nonlinear membrane behaviour would ultimately be required.

*Acknowledgments*—This research was supported by NIH grants HL11307, HL40609, the Heart and Stroke Foundation of Alberta and the Alberta Heritage Foundation for Medical Research. The work by Robert Plonsey was performed while on sabbatical leave at the Division of Biomedical Engineering of the University of Twente, Enschede, the Netherlands. The authors express their thanks to the Division Director, Professor Herman K. Boom, who read the manuscript and made several helpful suggestions. Gratitude is also owed to Ms Lianne Cartee for many suggestions and corrections.

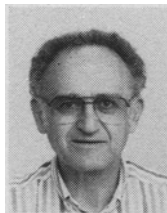
#### References

- CHAPMAN, L. A. and FRY, C. H. (1978) An analysis of the cable properties of frog ventricular myocardium. *J. Physiol.*, **283**, 263–282.
- DOLBER, P. C. and SPACH, M. S. (1987) Thin collagenous septa in cardiac muscle. *Anat. Rec.*, **218**, 45–55.
- HESCHELER, J. and SPEICHER, R. (1989) Regular and chaotic behavior of cardiac cells stimulated at frequencies between 2 and 20 Hz. *Eur. Biophysics J.*, **17**, 273–280.
- IDEKER, R. E., CHEN, P.-S., SHABITA, N., COLAVITA, P. G., WHARTON, J. M. (1987) Current concepts of the mechanisms of ventricular defibrillation. In *Nonpharmacological therapy of tachyarrhythmias*, BREITHARDT, G., BORGGREFE, M., and ZIPES, D. P. (Eds), Futura Publishing Company, Mount Kisco, New York.
- PLONSEY, R. and BARR, R. C. (1986a) Effect of microscopic and macroscopic discontinuities on the response of cardiac tissue to defibrillating (stimulating) currents. *Med. & Biol. Eng. & Comput.*, **24**, 130–136.
- PLONSEY, R. and BARR, R. C. (1986b) Inclusion of junction elements in a linear cardiac model through secondary sources:

application to defibrillation. *Med. & Biol. Eng. & Comput.*, **24**, 137-144.

- PLONSEY, R. and BARR, R. C. (1988) *Bioelectricity—a quantitative approach*. Plenum Press, New York.
- SCHUDER, J. C., STOECKLE, H., MCDANIEL, W. C. and DBEIS, M. (1987) Is the effectiveness of cardiac ventricular defibrillation dependent upon polarity? *Med. Instrum.*, **21**, 262-265.
- STREETER, D. (1979) *Handbook of Physiology*, Section 2, Vol. 1, 61-112.
- WEIDMANN, S. (1970) Electrical constants of trabecular muscle from mammalian heart. *J. Physiol.*, **210**, 1041-1054.
- WITKOWSKI, F. X., PENKOSKE, P. A. and PLONSEY, R. (1990) Mechanism of cardiac defibrillation in open chest dogs using unipolar dc-coupled simultaneous activation and shock potential recordings, *Circulation*, **82**, 244-260.

### Authors' biographies



Dr. Robert Plonsey received the BSEE from Cooper Union in 1943, the MSEE from NYU in 1948 and the Ph.D. in Electrical Engineering from the University of California, Berkeley, in 1956. After professorships in Electrical Engineering (1957-1968) and Biomedical Engineering (1968-1983) at Case Western Reserve University, he became Professor of Biomedical Engineering at Duke University in 1983. His research interests centre on the application of quanti-

tative models to problems in electrocardiography and cardiac electrophysiology. Dr. Plonsey is active in the IEEE EMBS, the US BES and is a member of the American Physiological Society.



Roger C. Barr is Professor of Biomedical Engineering and Associate Professor of Pediatrics at Duke University, where he has been on the faculty since 1969. His research interests include problems in electrocardiography, electrophysiology and biomedical computing.



Francis X. Witkowski was born in Brooklyn, New York, in 1947. He received the BS degree in electrical engineering from Manhattan College in 1969, the MS degree in Electrical Engineering from Northeastern University in 1972 and the MD degree from Washington University in 1978. Since 1984 he has been on the University of Alberta School of Medicine faculty, and is currently an Associate Professor of Medicine and a Scholar of the Alberta Heritage Foundation for Medical Research. His main research interests are in the design and application of cardiac mapping systems with a focus on ventricular fibrillation and defibrillation.